

# Synthesis of Some Baria-Modified $\gamma$ -Al<sub>2</sub>O<sub>3</sub> for Methanol Dehydration to Dimethyl Ether

Safae Hoda, Sohrabi Morteza\* and Falamaki Cavus

Chemical Engineering Department, Amirkabir University of Technology, Hafez Avenue, Tehran 15914, IRAN

Available online at: [www.isca.in](http://www.isca.in)

Received 26<sup>th</sup> September 2012, revised 10<sup>th</sup> October 2012, accepted 22<sup>nd</sup> November 2012

## Abstract

*In the present study a kinetic model for the catalytic dehydration of methanol to dimethyl ether, using some baria-modified gamma alumina as the reaction catalyst have been presented. Three catalyst samples were prepared consisting of Ba<sup>2+</sup> impregnated on  $\gamma$ -Al<sub>2</sub>O<sub>3</sub>, using barium nitrate solution. It was noted that the Ba<sup>2+</sup> content of the catalysts had a high impact on the activity of the latter. The operating temperature range was 260-290 °C and the pressure was 1 bar. Catalysts' activity and kinetic measurements were carried out using a catalytic fixed bed micro- reactor.*

**Keywords:** Modified  $\gamma$ -Al<sub>2</sub>O<sub>3</sub>, methanol dehydration, dimethyl ether.

## Introduction

Owing to the increasing air pollution during the last decade, and imposing of tougher environmental regulations, dimethyl ether (DME) has received global attention due to its potential use as a clean alternative fuel for diesel engines. In addition DME is an intermediate in the preparation of a number of industrial chemicals<sup>1-3</sup>.

DME can be produced from either of the following two methods: i. a single step process, that is the direct formation of DME from synthesis gas over hybrid catalysts and ii. dehydration of methanol over solid acid catalysts<sup>4-14</sup> according the following reaction:



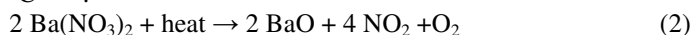
Among the solid acid catalysts used for methanol dehydration,  $\gamma$ -Al<sub>2</sub>O<sub>3</sub> has been studied intensively for both academic and commercial purposes<sup>15-18</sup>. However, this compound is normally sintered during a relatively long period of application. As sintering is the most serious cause of gamma alumina deactivation; the main purpose of the present study, was to prepare some catalysts with longer life times and lower operating temperature. Three catalyst samples were prepared, characterized and tested. The sample with the highest activity was considered as a suitable catalyst.

## Material and Methods

The chemicals used in the present study were all analytical grades and supplied by Merck, BASF and Condea Plural, Germany. These were barium nitrate [Ba(NO<sub>3</sub>)<sub>2</sub>], Methanol,  $\gamma$ -Al<sub>2</sub>O<sub>3</sub> and Pseudo boehmite.

**$\gamma$ -Al<sub>2</sub>O<sub>3</sub>:** Gamma aluminawas prepared by thermal decomposition of the pseudo boehmite precursor at 600 °C for 20 min, applying a heating rate of 20 °C/min.

**$\gamma$ -Al<sub>2</sub>O<sub>3</sub> modification:** Introduction of BaO to  $\gamma$ -Al<sub>2</sub>O<sub>3</sub> should be performed up to an optimum value. It is well known that BaO largely inhibits the  $\gamma \rightarrow \alpha$  phase transition<sup>19</sup>. In addition, excess BaO reduces the catalyst's surface area leading to the reduction of catalytic activity. As the purpose of this work containing various amounts of barium oxide (0.1, 1, 5 wt%) were prepared. Barium oxide was impregnated to  $\gamma$ -Al<sub>2</sub>O<sub>3</sub> by first dissolving the barium nitrate, in deionized water (100 ml) and mixing the latter with an aqueous suspension of  $\gamma$ -Al<sub>2</sub>O<sub>3</sub> (10 g) in deionized water (200 ml). The slurry was then stirred for 3h, and gradually dried in a rotary evaporator at 70 °C for 3h, to avoid segregation of impregnated nitrate. Heating of the sample was continued over night, in an oven at 110 °C, before being calcined at 535 °C for 1h, to remove hydroxyl water and nitrate. The nitrates of divalent cations generally decompose to corresponding oxides at relatively low temperature, around 500 °C<sup>20-21</sup>.



The ratio of barium oxide to  $\gamma$ -Al<sub>2</sub>O<sub>3</sub> was fixed at 0.1, 1 and 5 wt%. These samples and the one containing no barium oxide were analyzed by STA test (TGA+DTA) to determine and compare the transformation temperature.

Figure 1a and b shows the DTA and TG curves of the raw and modified  $\gamma$ -Al<sub>2</sub>O<sub>3</sub> samples containing various amounts of BaO. The exothermic transition peaks were observed at 1209 and 1216 °C for the raw sample and the one modified with 0.1 wt% BaO, respectively, whereas no exothermic transition peak was detected in case of other samples. These measurements were conducted using STA equipment, model PLSTA. In case of TG measurements, a heating rate of 10°C.min<sup>-1</sup> under continuous flow of air was applied. The sample's weight was 10 mg. In TG curve for the sample containing 0.1 wt% barium nitrate an endothermic peak was observed around 200°C. This may be related to the loss of hydroxyl water and nitrate<sup>20</sup>.

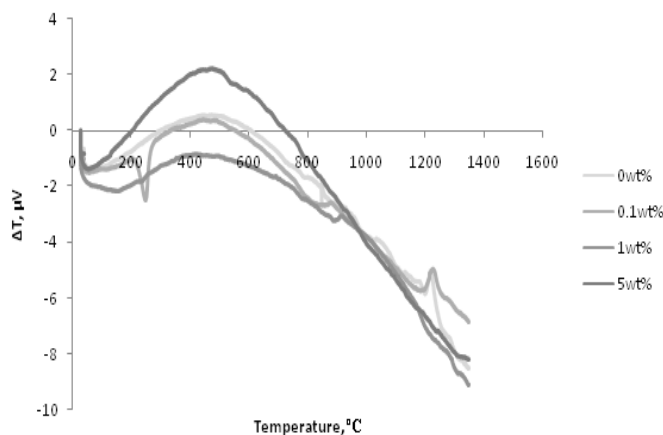


**Figure-1a**  
DTA curves of different sample

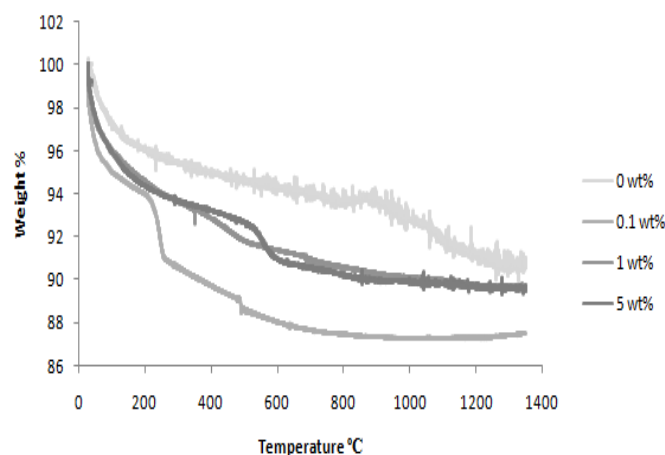


**Figure-1b**  
TG curves of different samples

As the rest of the samples had been dried before the DTA test, such a peak was not appeared in TG curves of the latter. In case of the sample containing 5wt% of barium nitrate, a peak was observed around 500°C. This could be due to the barium nitrate decomposition to BaO at such a temperature<sup>19</sup>. Such a peak was not significant for all other samples as they had been dried at high temperature before the STA test.

STA measurements demonstrated that a content of 0.1 wt% BaO retarded the  $\gamma$  to  $\alpha$  phase transition about 7°C, while larger contents shifted the transition temperature to higher than 1400 °C. The results are given in table 1. Based on the catalytic performance of the samples, it was deduced that addition of 1wt% BaO increases the life time of catalyst while maintaining a reasonable catalyst activity. The results are shown in table 1.

**Catalytic Activity:** Catalytic activity of the selected samples was studied under steady state conditions in a fixed bed reactor (16 mm i.d. and 70 cm length) equipped with an on-line GC apparatus. Experimental runs were all performed at atmospheric pressure, and a temperature of 260°C. As previous studies on  $\gamma$ -

$\text{Al}_2\text{O}_3$  activity have shown that with particles smaller than 0.17 mm in size the intra-particle resistances are negligible<sup>22</sup>, prior to catalytic testing, the samples were pressed, crushed and then sieved to 0.11 mm pellets. In each experiment, 1 g of the catalyst was loaded to the reactor and fixed between two quartz packing (0.01 mm in size) at both ends of the catalyst bed. Nitrogen saturated with pure methanol (0.35 bar partial pressure of methanol in nitrogen) was used as the feed, with a flow rate of 665.57  $\text{cm}^3 \text{min}^{-1}$ . The catalyst was first activated at atmospheric pressure and temperature of 410°C for 1h, applying a flow of nitrogen gas with the rate of 100  $\text{cm}^3 \text{min}^{-1}$ . The nitrogen flow rate was then increased to 665.57  $\text{cm}^3 \text{min}^{-1}$  with simultaneous decrease in temperature to 260°C. When a stable temperature was established, methanol was injected to the nitrogen stream with a flow rate of 0.6  $\text{cm}^3 \text{min}^{-1}$ . After steady state conditions were prevailed within the system (about 45 min), analysis of the outlet gas from the reactor was performed using a GC online apparatus. The results are shown in table 2.

In order to examine the stability and activity of the catalyst containing 1wt% BaO during a long period of application, an experimental run was performed using such a catalyst for 120 h time on stream. It was found that neither structure nor activity of the sample was affected during this period. Based on such an observation, it was deduced that addition of 1wt% BaO increases the life time of catalyst while maintaining a reasonable catalytic activity.

**Table-1**  
Phase transformation temperatures of the catalyst samples

Samples	Raw. $\gamma$ - $\text{Al}_2\text{O}_3$	0.1 wt%	1 wt%	5 wt%
Phase transformation Temperature °C	1206	1216	>1400	>1400

**Table-2**  
Methanol conversion on different catalyst samples

	Raw. $\gamma$ - $\text{Al}_2\text{O}_3$	Commercial $\gamma$ - $\text{Al}_2\text{O}_3$	0.1wt %	1 wt%	5 wt%
Methanol conversion	28.34	28.42	25.56	21.31	7.3

## Results and Discussion

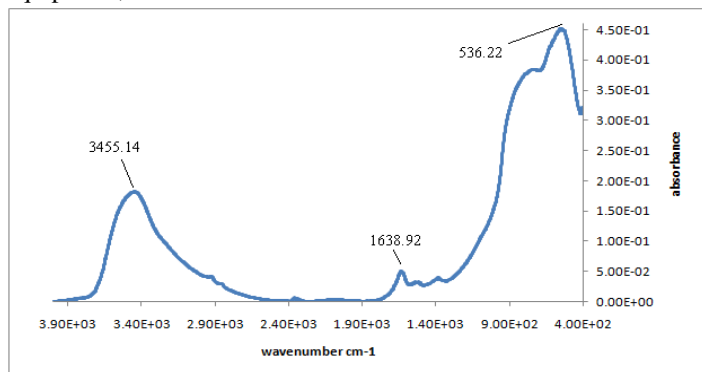
**Catalyst Characterization:** The raw  $\gamma$ - $\text{Al}_2\text{O}_3$  catalyst and the modified sample with 1wt% BaO were characterized applying BET, FTIR, XRD and SEM analyses. The BET specific surface area of the 1wt% modified sample and raw  $\gamma$ - $\text{Al}_2\text{O}_3$  are given in table 3.

**Table-3**  
BET specific surface area

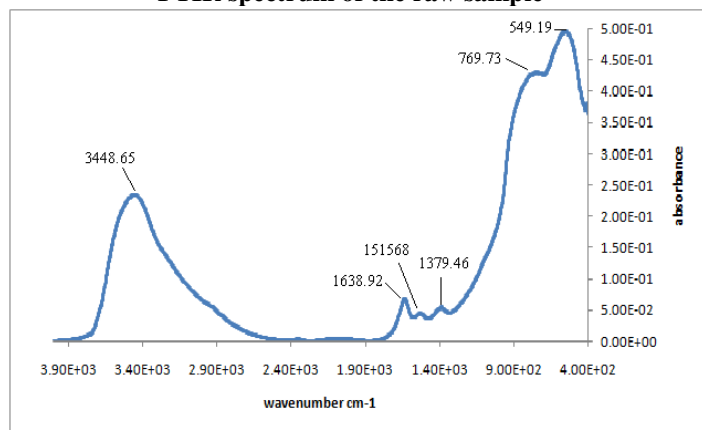
0 wt%	1 wt%	Catalyst sample
200	143.2	BET result ( $\text{m}^2/\text{g}$ )

As it is apparent from the table, the BET of the modified sample is less than that of the raw  $\text{Al}_2\text{O}_3$ . This may be due to the presence of large BaO molecules in the modified sample.

The FTIR spectra of the raw and modified catalysts are shown in figure 3a and b. The raw catalyst shows an adsorption band in a region close to  $3455.14\text{ cm}^{-1}$ . The bands around this region are usually attributed to bridging hydroxyls (free bridging or Bronsted acid sites). On the other hand, the Lewis acid sites appeared in  $1465\text{ cm}^{-1}$ <sup>23</sup>. It is evident that the number of both acid types in modified catalyst is higher than that of the raw sample. This analysis was carried out using a Nicolet FTIR equipment, model NEXUS 70 EP.

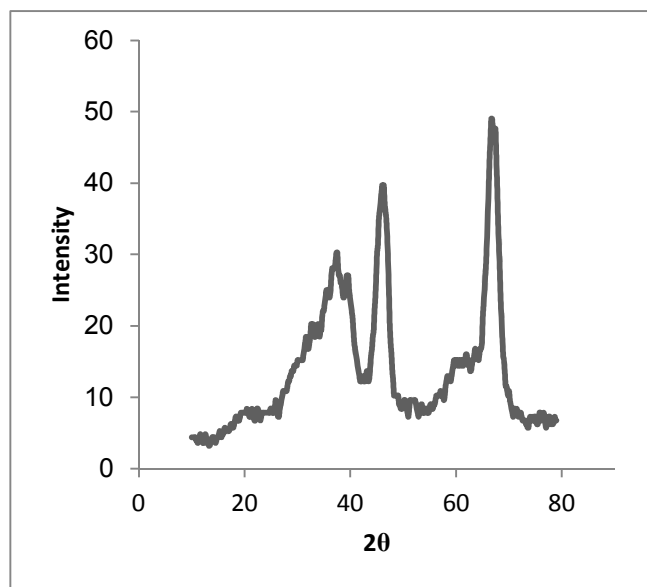


**Figure-3a**  
FTIR spectrum of the raw sample



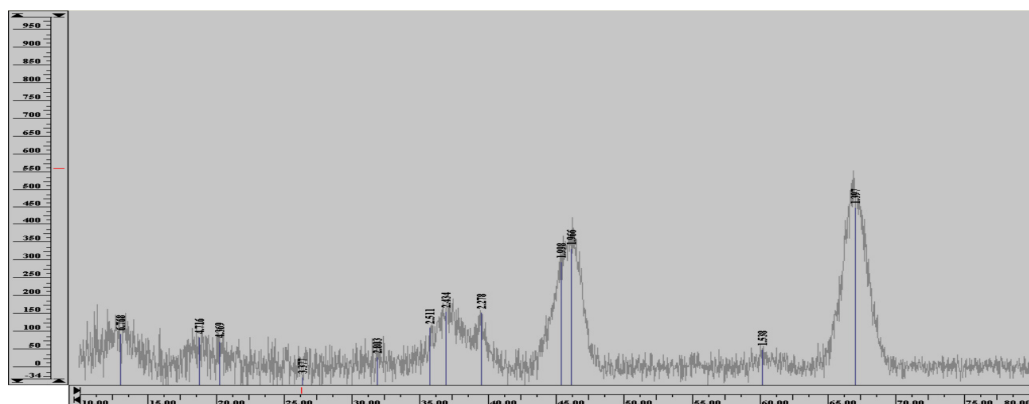
**Figure-3b**  
FTIR spectrum of the modified sample

Figure 4a and b demonstrates the XRD patterns of the raw and modified  $\gamma\text{-Al}_2\text{O}_3$ <sup>24</sup>. The peaks appeared at  $2\theta$  close to 26, 34 and 45 are related to BaO. The X-ray analysis have been carried out applying a Philips X-ray diffractometer, model XPERT.



**Figure-4a**  
X-Ray diffractometry of raw sample, the peaks appeared at  $2\theta = 13.85, 36.89, 39.77, 46.49$  and  $66.65$  are related to  $\gamma\text{-Al}_2\text{O}_3$ <sup>24</sup>

The microstructure of raw  $\gamma\text{-Al}_2\text{O}_3$  and modified catalyst containing 1 wt% BaO was revealed by scanning electron microscopy analysis (Philips SEM, model XL30). As it may be observed from figure 5a and b, presence of about 1 wt% of BaO in the samples retards the sintering of  $\gamma\text{-Al}_2\text{O}_3$  particles. Prior to the SEM analysis, the samples were prepared as small tablets and heated in a furnace for 1h at  $1400^\circ\text{C}$ .



**Figure-4b**  
The X-Ray diffractometry of the modified sample

Kinetic investigation: The process conditions applied in the kinetic investigations and the conversions of methanol are presented in table 4. A plug flow was assumed for the gas phase within the reactor.

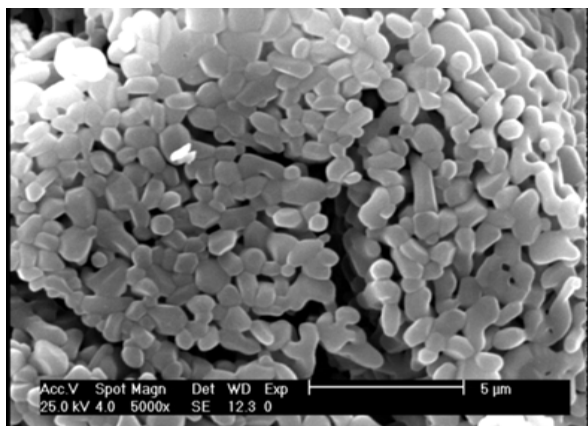


Figure-5a  
SEM of the raw sample

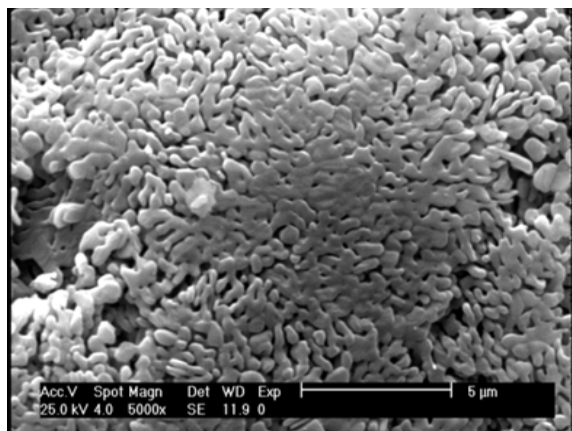
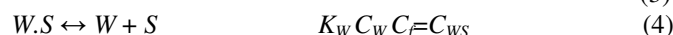


Figure-5b  
SEM of the modified sample

A number of studies on methanol dehydration to DME have been carried out, including those of Bercic and Levec (1992, 1993) Royae et al (2008). Both Eley-Rideal and Langmuir-

Hinshelwood type mechanisms have been proposed for the catalytic dehydration reaction of methanol<sup>25-29</sup>. A kinetic model based on Langmuir-Hinshelwood surface controlled reaction with dissociative adsorption of methanol, neglecting adsorption term for DME, was found to be well correlated with the experimental results. In this model the term describing the reversible nature of the reaction was disregarded. This was due to the identical results obtained with and without considering the latter term in the kinetic model. The reaction mechanism proposed is as follows,



Leading to the following model,

$$R_M = \frac{k K_M^2 C_M^2}{[1 + 2(K_M C_M)^{0.5} + K_W C_W]^4} \quad (5)$$

Where, M, W and D stand for methanol, water and DME, respectively; S, is the active site;  $K_M$  and  $K_W$ , are the adsorption coefficients of methanol and water, respectively;  $C_M$ ,  $C_W$  and  $C_f$  are concentrations of methanol, water and free active sites, respectively;  $R_M$ , is the rate of methanol dehydration;  $k$ , is the rate coefficient;  $C_{MS_2}$  and  $C_{WS}$ , are the concentrations of methanol and water adsorbed on the active sites. Table 5 shows the optimized parameters for the reaction scheme presented.

A comparison has been made between the experimental data for DME concentrations and those predicted from the model as shown in figure 6. The mean absolute deviation is within the range of 6-10%.

Table-4  
The process parameters and measured conversion of methanol

MeOH (mol%)	MeOH flow rate (cm <sup>3</sup> min <sup>-1</sup> )	Nitrogen flow rate (cm <sup>3</sup> min <sup>-1</sup> )	Conversion at 260°C	Conversion at 280°C	Conversion at 290°C
20	0.30	716.76	27.73	39.73	46.33
27.5	0.45	691.165	24.38	34.49	40.02
35	0.60	665.57	21.31	29.90	36.85
42.5	0.75	601.705	17.55	27.85	34.51
50	0.90	537.84	15.44	25.23	31.70

Table-5  
Optimal calculated parameters for reaction

$K_W$ (m <sup>3</sup> /kmol)	$K_M$ (m <sup>3</sup> /kmol)	K (kmol/hr)	Temperature
739.68	21.13	0.66	260 °C
560.11	11.5	2.76	280 °C
384.2	9	5.5	290 °C

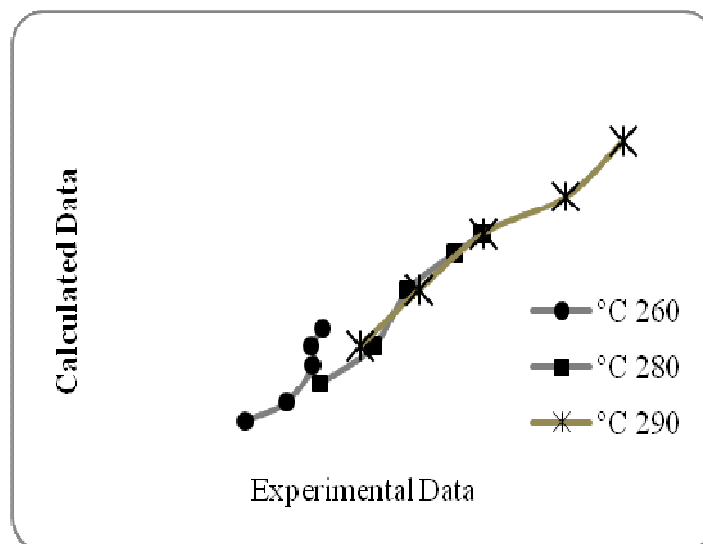


Figure-6  
Calculated data versus experimental data of DME outlet concentrations

## Conclusion

Analysis of the synthesized catalysts revealed that modification of  $\gamma\text{-Al}_2\text{O}_3$  by 1 wt% barium oxide imposed a high resistance to phase transition and sintering of the catalyst<sup>17</sup>. A comparison was made between the performance capability of the raw and modified  $\gamma\text{-Al}_2\text{O}_3$  in dehydration of methanol under identical operating conditions ( $T=260\text{ }^\circ\text{C}$ ,  $P=1\text{ bar}$ , methanol partial pressure= 0.35 bar). As it is apparent from the present results, with both raw and modified  $\gamma\text{-Al}_2\text{O}_3$  at low temperatures and pressure, reasonable methanol conversions are obtained. Lower temperature and pressure mean lower energy consumption and thus, less expenses. Decrease in conversion of methanol with application of  $\gamma\text{-Al}_2\text{O}_3$  impregnated with 1wt% barium oxide in comparison with raw  $\gamma\text{-Al}_2\text{O}_3$  may be completely compensated by increase in life time of modified  $\gamma\text{-Al}_2\text{O}_3$ . Application of this catalyst is, therefore, recommended for high capacity industrial reactors for methanol dehydration to dimethyl ether.

Also the kinetic behavior of 1 wt% modified  $\gamma\text{-Al}_2\text{O}_3$  for the MTD reaction had been investigated using a fixed bed microreactor and a Langmuir-Hinshelwood model was presented.

## Reference

1. Hansen J., Voss B., Joensen F. and Siguroavdottir I., Large scale manufacture of dimethyl ether a new alternative diesel fuel from natural gas, in: SAE Technical Paper Series, International Congress and Exposition, Detroit, Michigan, February 27-March 2, (1995)
2. Kasai M. and Sohrabi M., Kinetic study on methanol dehydration to dimethyl ether applying Clinoptilolite zeolite as the reaction catalyst, *J. Mex. Chem. Soc.*, **53**, 233-238 (2009)
3. Fleisch T., McCarthy C., Basu A., Udovich C., Charbonneau P., Slodowske W., Mikkelsen S. and McCan-dless J.M., A New Clean Diesel Technology: Demonstration of ULEV Emissions on a Navistar Diesel Engine Fueled with Dimethyl Ether (1995)
4. Sonawane Vilas Y., Mechanistic study of chromium (VI) catalyzed oxidation of benzyl alcohol by polymer supported chromic acid, *Res. J. Chem. Sci.*, **1**(1), 25-30 (2011)
5. Kumar V., Mangain R. and Singh N., Synthesis of substituted imidazoles via a multi-component condensation catalyzed by *p*-toluene sulfonic acid, PTSA, *Res.J.Chem.Sci.*, **2**(4), 18-23 (2012)
6. Kannan C., Devi M.R., Muthuraja K., Esaivani K. and Sudalai Vadivoo V., Green catalytic polymerization of styrene in the vapor phase over alumina, *Res.J.Chem. Sci.*, **2**(7), 27-35 (2012)
7. Deepshikha and Basu T., The Role of Structure Directing Agents on Chemical Switching Properties of Nanostructured Conducting Polyaniline (NSPANI), *Res.J.Chem.Sci.*, **1**(6), 20-29 (2011)
8. Deshpande D.P., Urunkar Y.D and Thakare P.D., Production of biodiesel from castor oil using acid and base catalysts, *Res.J.Chem.Sci.*, **2**(8), 51-56 (2012)
9. Deshpande D.P., Warfade V.V., Amaley S.H. and Lokhande D.D., Petro-Chemical Feed stock from Plastic Waste, *Res.J.Recent Sci.*, **1**(3), 63-67 (2012)
10. Tandel R.C., Jayvirsinh G. and Patel Nilesh K., Synthesis and study of main chain chalcone polymers exhibiting nematic phases, *Res.J.Recent.Sci.*, **1**, 122-127 (2012)
11. Anju S.G., Jyothi K.P., Sndhu J., Suguna Y. and Yesodharan E.P., Ultrasound assisted semiconductor

- mediated catalytic degradation of organic pollutants in water: comparative efficacy of ZnO, TiO<sub>2</sub> and ZnO-TiO<sub>2</sub>, *Res.J.Recent.Sci.*, **1**, 191-201 (2012)
12. Femina P. and Sanjay P., Carbon monoxide on LaCoO<sub>3</sub> perovskite type catalysts prepared by reactive grinding, *Res.J.Recent.Sci.*, **1**, 152-159 (2012)
  13. Femina P. and Sanjay P., LaCoO<sub>3</sub> perovskite catalysts for the environmental application of auto motive CO oxidation, *Res.J.Recent.Sci.*, **1**, 178-184 (2012) with dimethyl ether, in SAE Technical Paper Series, Interational Congress & Exposition, Detroit, Michigan, February 27-March 2, (1995)
  14. Nle Z., Liu H., Ying W. and Fang D., Intrinsic kinetics of dimethyl ether synthesis from syngas, *J. Nat. Gas Chem.*, **14**, 22-28 (2005)
  15. Woodhouse J.C, US Patent 2, 014, 408 (1935)
  16. Topp-Jorgensen J., US Patent 4, 536, 485 (1985)
  17. Vishwanathan V., Jun K., Kim J. and Roh H.J., Vapour phase dehydration of crude methanol to dimethyl ether over Na-modified H-ZSM-5 catalysts, *App. Catal. A*, **276**, 251-255 (2004)
  18. Knözinger, Kochloefl K. and Meye W., Kinetics of the biomolecular ether formation from alcohols over alumina, *J. Catal.*, **28**, 69-75 (1973)
  19. Okada K. and Hattori A., Effect of divalent cation additives on the  $\gamma$ -Al<sub>2</sub>O<sub>3</sub>-to- $\alpha$ -Al<sub>2</sub>O<sub>3</sub> phase transition, *J. Am. Ceram. Soc.*, **83**, 928-932 (2000)
  20. Okada K., Hattori A., Kameshima Y. and Yasumori A., Effect of monovalent cation additives on the  $\gamma$ -Al<sub>2</sub>O<sub>3</sub>-to- $\alpha$ -Al<sub>2</sub>O<sub>3</sub> phase transition, *J. Am. Ceram. Soc.*, **83**, 1233-1236 (2000)
  21. Saito Y., Takei T., Hayashi S., Yasumori A. and Okada K., Effects of amorphous and crystalline SiO<sub>2</sub> additives on  $\gamma$ -Al<sub>2</sub>O<sub>3</sub>-to- $\alpha$ -Al<sub>2</sub>O<sub>3</sub> phase transitions, *J.Am. Ceram. Soc.*, **81**, 2197-2200 (1998)
  22. Bercic G. and Levec J., Intrinsic and global reaction rate of methanol dehydration over  $\gamma$ -Al<sub>2</sub>O<sub>3</sub> pellets, *Ind. Eng. Chem. Res.*, **3**, 1035-1040 (1992)
  23. Royae S.J., Falamaki C. and Sohrabi M., A new Langmuir Hinshelwood mechanism for the methanol to dimethyletherreaction over clinoptilolite zeolite catalyst, *J. Applied Catalysis A: General*, **338**, 114-120 (2008)
  24. Okada A., Yamaguchi T. and Fujita T., Cation dopant effect on phase transformation and microstructural evolution in M<sup>+2</sup>- substituted  $\gamma$ -alumina powders, *J. Mater Sci.*, **43**, 2713-2720 (2008)
  25. Bandiera J. and Naccache C., Kinetics of methanoldehydration on dealuminated H-mordenite: Model withacid and basic active centers, *J. Appl. Catal.*, **69**, 139-148 (1991)
  26. Bercic G. and Levec J., Catalytic dehydration of methanol to dimethyl ether. Kinetic investigation and reactor simulation, *Ind. Eng. Chem. Res.*, **32**, 2478-2484 (1993)
  27. Schmitz G., Deshydration du methanol sur silice- alumina, *Chem. Phys.*, **75**, 650-655 (1978)
  28. Gates B.C. and Johanson L.N., Metal clusters in catalysis, *AIChE J.*, **34**, 173-174 (1998)
  29. Hadipour A. and Sohrabi M., Synthesis of some bifunctional catalysts and determination of kinetic parameters for direct conversion of syngas to dimethyl ether, *J. Chem. Eng.*, **137**, 294-301 (2008)